8-22-2006

Binding of Internalized Receptors to the PDZ Domain of GIPC/Synectin Recruits Myosin VI to Endocytic Vesicles

Samia N. Naccache
University of California - San Diego

Tama Hasson
University of California - San Diego

Arie Horowitz
Dartmouth College

Binding of internalized receptors to the PDZ domain of GIPC/synectin recruits myosin VI to endocytic vesicles

Samia N. Naccache*, Tama Hasson*†, and Arie Horowitz‡§

*Section of Cell and Developmental Biology, Division of Biological Sciences, University of California at San Diego, La Jolla, CA 92093; †College of Letters and Science, Undergraduate Research Center/Center for Academic and Research Excellence, University of California, Los Angeles, CA 90095; and ‡Angiogenesis Research Center and Section of Cardiology, Dartmouth Medical School, Lebanon, NH 03756

Communicated by Marilyn Gist Farquhar, University of California at San Diego School of Medicine, La Jolla, CA, July 6, 2006 (received for review November 11, 2005)

Myosin VI (myo6) is the only actin-based molecular motor that translocates along actin filaments toward the minus end. Myo6 participates in two steps of endocytic trafficking; it is recruited to both clathrin-coated pits and to ensuing uncoated endocytic vesicles (UCV). Although there is evidence suggesting that the PDZ adaptor protein GIPC/synectin is involved in the association of myo6 with UCV, the recruitment mechanism is unknown. We show that GIPC/synectin is required for both internalization of cell surface receptors and for coupling of myo6 to UCV. This coupling occurs via a mechanism wherein engagement of the GIPC/synectin PDZ domain by C termini of internalized receptors facilitates *in trans* myo6 binding to the GIPC/synectin C terminus located outside of the PDZ domain. Analysis of megalin, a prototypical GIPC/synectin-binding receptor, revealed that deletion of its PDZ-binding motif drastically reduced GIPC/synectin and myo6 recruitment to UCV. Furthermore, interaction with GIPC/synectin was required for megalin's function, as megalin was mistargeted in the renal proximal tubules of GIPC/synectin-null mice and these mice exhibited proteinuria, a condition consistent with defective megalin trafficking.

traffic | molecular motor | kidney

Unconventional myosins are actin-based molecular motors implicated in vesicle and organelle movement (1–3). Myosins are comprised of two major domains: the highly conserved motor domain that binds F-actin and converts energy from ATP hydrolysis into directional motion along the actin filament, and the divergent tail domain that mediates cargo binding and can contain a variety of protein–protein and protein–lipid interaction motifs. Although associations between the myosins and their cargoes are tail-specific, the mechanisms that govern the recruitment of myosins to their cargoes have not yet been fully determined.

Myosin VI (myo6) is involved in endocytic transport (4, 5) and is the only actin-based molecular motor that translocates along actin filaments toward the minus end (6). In the cell, actin filaments are predominantly oriented with minus ends pointed inward, supporting a role for myo6 in endocytic trafficking. Indeed, the emerging picture is that myo6 participates in two steps of trafficking as it is recruited to both clathrin-coated pits (CCP) and the ensuing uncoated endocytic vesicles (UCV) (7–9).

Myo6 associates with CCP via the adapter protein Dab2 (5). Dab2 binds directly to clathrin, to the clathrin adaptor protein AP-2 (10) and to myo6 (11, 12). The protein likely involved in UCV recruitment, however, is GIPC (GAIP interacting protein, C terminus) (13), a single Postsynaptic density 95, Disks large, Zona occludens-1 (PDZ) domain adaptor protein also denoted as synectin (14). Synectin's central PDZ domain binds type I PDZ-binding motifs (PBMs) conforming to the consensus sequence (S/T)-X-(V/A) (15). Synectin is one of the most versatile PDZ proteins known to date, with 25 binding partners, most of which are transmembrane receptors or adhesion molecules (e.g., refs. 14, 16, and 17).

Synectin captured the tail domain of myo6 in a yeast two-hybrid screen (18). Synectin interacts with myo6 *in vivo* as the two proteins collocate on UCV and can be coimmunoprecipitated from membrane fractions (7). A portion of the myo6 tail domain is sufficient to associate with UCV (7, 9). Myo6 is mainly found in a cytoplasmic pool, where it is not complexed with synectin or Dab2 (7), suggesting that its docking to cargo is regulated. However, the docking mechanism remains unknown.

We found that myo6 recruitment to UCV is synectin-dependent. PBM binding to the PDZ domain of synectin facilitated myo6 binding to a site in the C terminus of synectin located outside of the PDZ domain. We determined that deletion of the PBM of megalin, a known synectin-binding receptor (19), impaired synectin and myo6 recruitment to UCV. Finally, we found that synectin-null mice develop proteinuria, a condition consistent with defective megalin trafficking.

Results

Synectin Precedes myo6 on UCV. We considered two scenarios for myo6 recruitment to UCV: (*i*) synectin is required for myo6 recruitment to UCV, serving as an essential bridge to the UCV; (*ii*) synectin performs only an auxiliary role and is not required for myo6 recruitment. To test these alternatives, we took advantage of the *Snell's waltzer* (*sv*) mouse (20), which does not express myo6. In both wild type (WT) and *sv* kidney epithelial cells, synectin was evident on punctae that had all of the established identifiers of UCV (7): they did not collocate with markers for clathrin-coated vesicles (e.g., the clathrin-adaptor AP-2; data not shown), or with early endosome markers (e.g., EEA1; data not shown) but could be internally labeled with endocytosed rhodamine-conjugated EGF (R-EGF) after 2–4 min of endocytosis (Fig. 1 *A* and *B*). Moreover, at this time point, R-EGF was no longer present in CCP (data not shown), confirming that the R-EGF/synectin-labeled punctae were UCV. Peak R-EGF/synectin collocation occurred after 2 min at which 39.6 ± 5.5% and 42 ± 2% of the synectin-associated vesicles in WT and sv kidney cells, respectively, contained R-EGF. We concluded that myo6 was not required for synectin recruitment to the UCV surface.

The Presence of Both the N Terminus and the PDZ Domain of Synectin Is Required for Synectin Targeting to UCV. To identify the minimal region required for synectin targeting to UCV, we expressed a

Conflict of interest statement: No conflicts declared.

Abbreviations: CCP, clathrin-coated pits; UCV, uncoated endocytic vesicles; PBM, PDZ-binding motif; R-EGF, rhodamine-conjugated EGF; VFP, visual fluorescent protein; R-Tfn, rhodamine-conjugated transferrin; myo6, myosin VI.

§To whom correspondence should be addressed. E-mail: arie.horowitz@dartmouth.edu.

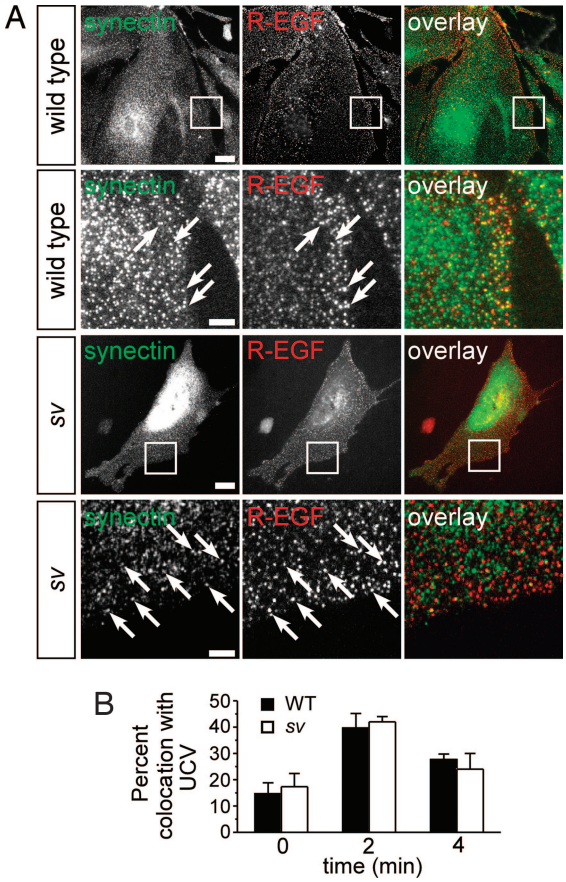

Fig. 1. Myo6 is not required for targeting of synectin to UCV. (*A*) Location of immunolabeled synectin (green) in WT and *sv* mouse kidney epithelial cells after 4 min uptake of R-EGF (red). Enlargements of boxed areas are shown in the bottom panels of each cell type. Collocated vesicles are indicated by arrows. (Scale bars: 10 μm; enlargements, 2.5 μm.) (*B*) Quantification of collocation in WT kidney epithelial cells (black bars) or *sv* cells (white bars) of R-EGF-containing vesicles and synectin-associated vesicles in a wide swath along the cell periphery. R-EGF was endocytosed by pulse–chase; cells were fixed at 0, 2, and 4 min of uptake. Synectin was detected by immunofluorescence. A total of 150 vesicles were counted from three different cells.

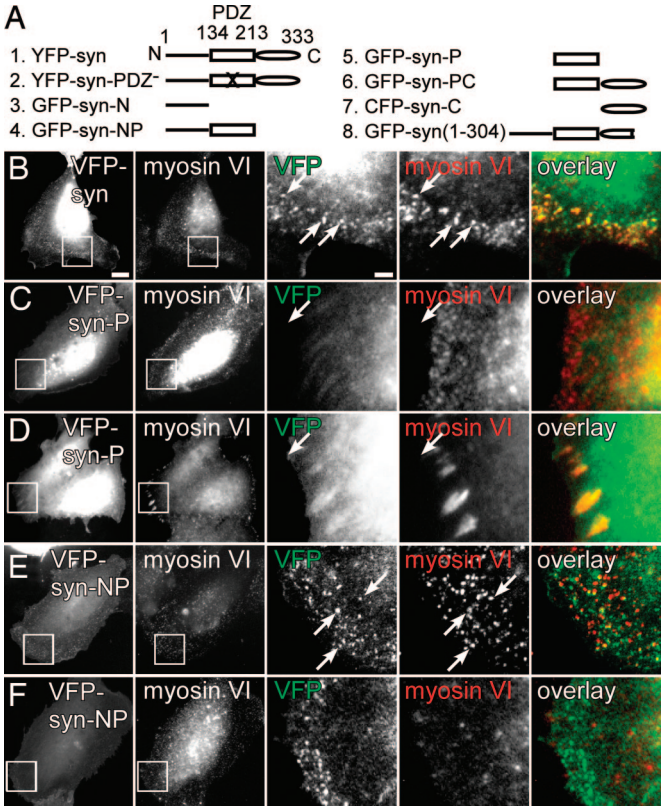

Fig. 2. The N-terminal and PDZ domains of synectin are required for UCV binding. (*A*) Schematic of GFP-, YFP-, and CFP-fused synectin constructs. Residue numbers at the ends of the N-terminal (N), PDZ (P), and C-terminal (C) domains are shown above the YFP-synectin construct. (*B–F*) ARPE-19 cells expressing VFP-fused synectin constructs (green). Boxed areas at *Left* are enlarged at *Right*. Furthermost *Right* is an overlay of the two magnified fields to its left. Vesicles showing collocation are indicated by arrows. (*B*) VFP-synectin-expressing cells stained for myo6 (rabbit-anti myo6, red) revealed significant collocation. (*C*) The PDZ domain (VFP-syn-P, green) was not recruited to UCV, and its expression did not interfere with myo6 targeting to vesicles in ARPE-19 cells (anti-myo6, red). (*D*) VFP-syn-P collocated with focal adhesion marker vinculin (red). (*E*) VFP-syn-NP targeted to peripheral vesicles internally labeled with R-Tfn (red) after 2-min pulse–chase uptake. (*F*) Expression of VFP-syn-NP (green) prevented myo6 (red) recruitment to UCV. (Scale bars: 10 μm; enlarged images, 2.5 μm.)

series of visual fluorescent protein (VFP, a generic term for GFP, CFP, and YFP)-tagged domain-deletion constructs of synectin in ARPE-19 cells, a human retinal epithelial cell line (Fig. 2*A* and Table 1). In ARPE-19 cells, UCV can also be labeled internally with rhodamine-conjugated transferrin (R-Tfn) 2 min after the initiation of endocytosis; at that time point, R-Tfn had exited CCP as it no longer collocated with the CCP markers AP-2 or clathrin (7) but had not yet reached the EEA1-positive early endosome (7, 9). Full-length VFP-synectin targeted specifically to UCV in ARPE-19 cells, where it collocated with R-Tfn after 2 min of pulse–chase uptake (Fig. 6*A*, which is published as supporting information on the PNAS web site) and with myo6 (Fig. 2*B* and Table 1) but did not collocate with AP-2 or EEA1 (Fig. 6 *B* and *C*).

Interestingly, the PDZ domain alone (VFP-syn-P) was not sufficient for UCV-association and its expression had no effect on myo6 targeting to UCV (Fig. 2*C*). Furthermore, VFP-syn-P did not collocate with endocytosed Tfn (data not shown). Instead, the PDZ domain was recruited to focal adhesions, overlapping with vinculin (Fig. 2*D*).

The smallest fragment of synectin capable of targeting to R-Tfn-containing UCV consisted of the N and PDZ domains (VFP-syn-NP; Fig. 2*E*). The UCV-targeting of this construct was as efficient as that of VFP-fused synectin; the extent of collocation of the two VFP-fused constructs with R-Tfn-containing vesicles after 2 min of pulse–chase uptake was virtually identical: 68.6 ± 7.57% and 68 ± 7.2%, respectively (Table 1). However, VFP-syn-N expressing the N terminus alone was diffusely distributed in the cytoplasm (Table

Table 1. Expression pattern of synectin constructs expressed in ARPE-19 cells and their overlap with R-Tfn and endogenous myo6 after 2-min pulse–chase uptake

Synectin construct	Expression pattern	Overlap with R-Tfn, %	Overlap with myo6, %
VFP-syn	UCV	68 ± 7.2	70 ± 2
VFP-syn-PDZ⁻	Diffuse	NA	NA
VFP-syn-N	Diffuse	NA	NA
VFP-syn-NP	UCV	68.6 ± 7.57	20.5 ± 8
VFP-syn-P	FA	None	3.00
VFP-syn-PC	FA	None	NA
VFP-syn-C	Diffuse	NA	NA

NA, not applicable; FA, focal adhesion.

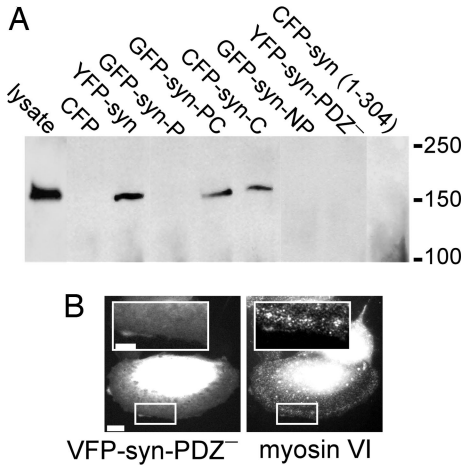

Fig. 3. Myo6 binding to the C terminus of synectin requires a functional synectin PDZ domain. (*A*) Myo6 immunoblot of ARPE-19 cell lysates transfected with the indicated synectin constructs and immunoprecipitated with anti-VFP (which recognizes all three GFP variants). Lysate lane was loaded with 10% of the immunoprecipitated sample volumes. Myo6 was coimmunoprecipitated only by synectin constructs that contained the full-length C-terminal domain. Coimmunoprecipitation was abolished by the deletion of the last 29 C-terminal residues [CFP-syn (1–304)] or by inactivation of the PDZ domain by two point mutations (X on the scheme of the YFP-syn-PDZ$^-$ construct in Fig. 2*A*). Numbers denote molecular mass in kilodaltons. (*B*) L142A/G143E (VFP-syn-PDZ$^-$) expression in ARPE-19 cells counterstained with anti-myo6. The PDZ domain mutations eliminated UCV recruitment, but had no effect on the targeting of endogenous myo6 to UCV. (Scale bars: 10 μm; *Inset*, 5 μm.)

1). Thus, both the N terminus and the PDZ binding domains, but not the C-terminal domain, are required and sufficient for synectin targeting to UCV (Table 1). Because the N-terminal domain self-associates (14, 21), dimerization appears to be required for synectin binding to UCV.

The myo6-Binding Site Is Located in the C Terminus of Synectin. Although VFP-syn-NP was capable of vesicle association, it apparently lacked the myo6-binding site as upon expression in ARPE-19 cells, myo6 was no longer recruited to UCV (Fig. 2*F*). Only 20.5 ± 8% of VFP-syn-NP punctae collocated with myo6, versus 70 ± 2% of VFP-synectin punctae (Table 1). Moreover, whereas R-Tfn endocytosis was normal (Fig. 2*F*), R-Tfn reached early endosomes only in 24.5 ± 6.2% of VFP-syn-NP-expressing cells after 15 min of uptake versus ≈90% of untransfected cells and cells expressing all other VFP-synectin constructs (Fig. 7 *A* and *B*, which is published as supporting information on the PNAS web site). This phenotype suggests a block in the inward transport of UCV and is similar to that seen upon expression of myo6 motor domain mutants (7). We concluded that the myo6-binding site is located in the C-terminal domain of synectin, and that VFP-syn-NP expression blocked trafficking by displacing endogenous synectin from UCV, thus preventing myo6 docking.

Coimmunoprecipitation experiments with a series of truncated synectin constructs narrowed down the location of the essential part of the myo6 binding motif to the last 29 residues in the C terminus (Fig. 3*A*). A construct lacking these residues no longer collocated with myo6 (data not shown).

A Functional PDZ Domain Is Required for Synectin Targeting to UCV. Uncoated endocytic vesicles carry numerous types of cell surface receptors from CCP to early endosomes. As a large number of transmembrane receptors bind to the PDZ domain of synectin, we hypothesized that this domain is required for synectin association with UCV. We replaced two consecutive residues in the carboxylate binding loop of synectin's PDZ domain (L142A/G143E), a mutation previously shown to impair the binding between synectin and Gα_i-interacting protein (17). When expressed in ARPE-19 cells, the mutant synectin (VFP-syn-PDZ$^-$) did not affect trafficking (Fig. 7*B*) and no longer targeted to UCV (Fig. 3*B*) confirming that UCV association requires binding of the PDZ domain of synectin to PBMs on the UCV surface.

Ligand Binding to the PDZ Domain of Synectin Facilitates myo6 Binding to the Synectin C Terminus. Surprisingly, although the VFP-syn-PDZ$^-$ construct possessed an intact myo6-binding site far removed from the two point mutations in the PDZ domain, it did not coimmunoprecipitate with myo6 (Fig. 3*A*, lane 8). We hypothesized that binding of the PDZ domain of synectin to its ligand on the UCV surface is required for myo6 binding to synectin and recruitment to UCV.

To determine the effect of ligand-binding to the PDZ domain on the interaction between synectin and myo6, we estimated the binding coefficients of the tail domain of myo6 to synectin in the presence of a peptide corresponding to the cytoplasmic tail of syndecan-4 (S4), previously shown to bind synectin (14). As a control, we used a syndecan-4 peptide lacking the C-terminal alanine (S4Δ), which does not bind synectin (22). Immobilized GST-fused myo6 tail domain (GST-M6tail) was used to pull down endogenous synectin from ARPE-19 cell lysates in the presence of each peptide (Fig. 8*A*, which is published as supporting information on the PNAS web site). We constructed saturation-binding curves to estimate the binding coefficients between myo6 and synectin under these conditions, by varying the fraction of ARPE-19 cell lysate in the constant total volume used in each pull-down experiment. The calculated dissociation constants in the presence of S4 or S4Δ were similar to each other: 1.2 and 1.7 nM, respectively (Fig. 8*B*). However, the B_{max} of the binding was more than twice larger in the presence of S4 than in the presence S4Δ (0.82 versus 0.35 nM·s^{-1}, respectively). These results suggest that ligand binding to the PDZ domain stabilizes synectin in a conformation favorable for myo6 binding. To further test the dependence of myo6 binding to synectin on engagement of the latter's PDZ domain, we repeated the pull-down on lysate of ARPE-19 cells expressing VFP-syn-PDZ$^-$. Although endogenous synectin was precipitated, GST-M6tail failed to bind and pull down VFP-syn-PDZ$^-$ (Fig. 8*C*).

Synectin-Null Mice Exhibit Proteinuria and Perturbed Megalin Targeting. The scavenger receptor megalin binds synectin (19) and collocates with it on the lumen of kidney proximal tubules (23) where myo6 is also located (24). Given the documented defects in the renal function of megalin-null mice (25), we sought to determine whether binding of megalin to synectin is essential for megalin's function in renal physiology. One of the renal defects found in megalin-null mice is low molecular weight proteinuria caused by tubular resorption deficiency (26). Urine analysis of synectin-null mice by SDS/PAGE revealed the presence of proteins which resolved into a band pattern similar to that of megalin-null mice. For example, urine from synectin-null mice contained retinol-binding protein (Fig. 4*A*), a known megalin ligand (27). However, the level of megalin found in the kidneys of synectin-null mice was equivalent to that seen in WT mice (Fig. 4*B*). The increased protein presence in the urine of synectin-null mice despite the normal expression of megalin in the proximal tubules of their kidneys suggested that megalin recycling is defective in these mice, and that synectin is required for proper megalin trafficking *in vivo*. Interestingly, myo6 expression level was 6-fold higher in synectin-null than in WT kidneys (Fig. 4*B*), reflecting a compensatory response to the impaired trafficking of megalin in the proximal tubules of synectin-null mice.

In WT mice (Fig. 4*C*) megalin was primarily detected in the endocytic region at the base of the proximal tubule cell mi-

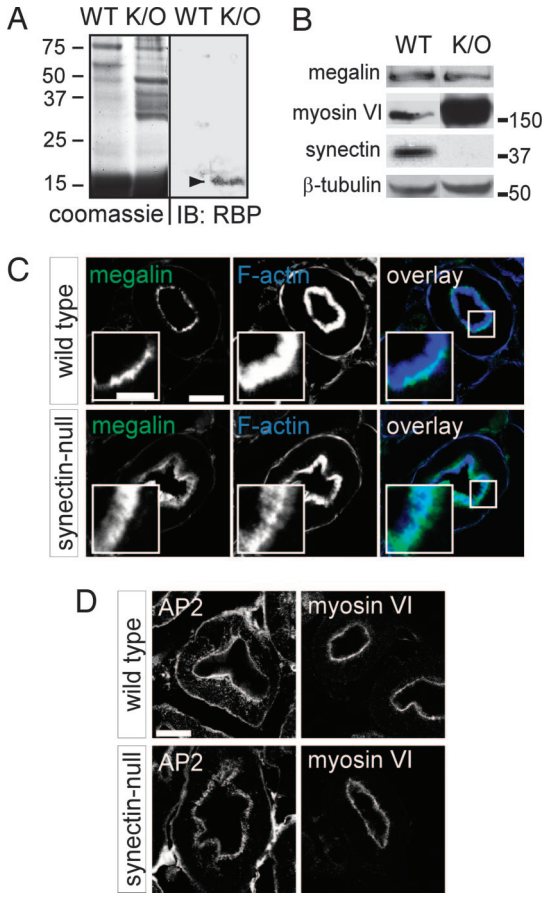

Fig. 4. Proteinuria and altered megalin distribution in synectin-null mice. (*A*) Coomassie-stained gel of urine samples from WT and from synectin-null mice revealed the presence of multiple bands in the synectin-null sample that were absent in the WT sample, indicative of proteinuria. Immunoblotting of similar urine samples detected the presence of the megalin ligand retinol-binding protein in the synectin-null urine sample. (*B*) Immunoblots of synectin, myo6, and megalin in WT and synectin-null mice. Fifty micrograms of total protein was loaded in each lane. The synectin-null myo6 band was ≈6-fold heavier than the WT one, as measured by densitometry. The β-tubulin immunoblot was used as a loading control. (*C* and *D*) Confocal images of 4-μm cryosections of WT and synectin-null mouse kidneys stained for megalin (green, *Left*) and F-actin (blue, *Center*) (*C*) or for AP-2 and F-actin (*D*). (Scale bars: 5 μm; *Inset*, 2.5 μm.)

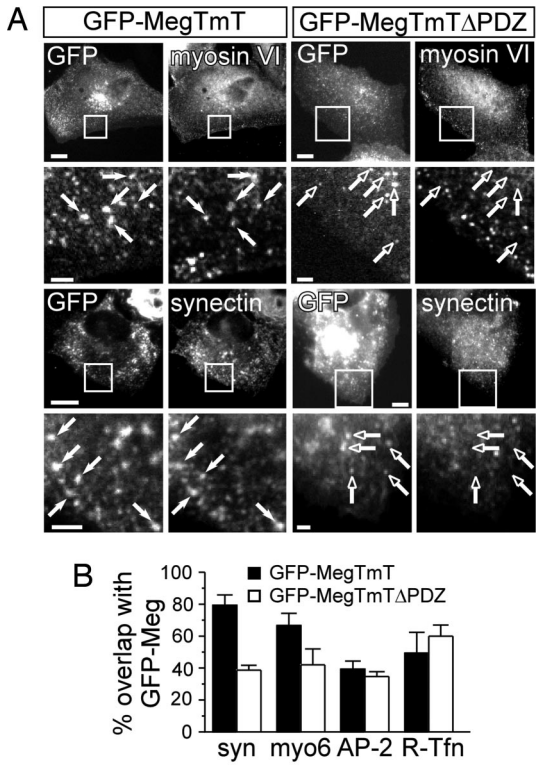

Fig. 5. Synectin binding to the PBM of megalin is required for synectin and myo6 recruitment to UCV. (*A*) Indirect immunofluorescence staining of ARPE-19 cells expressing GFP-MegTmT or GFP-MegTmTΔPDZ stained for myo6 or synectin. The second and fourth rows are enlargements of the boxed regions in the first and third rows. Filled arrows indicate collocation of GFP constructs, CFP constructs, and R-Tfn; open arrows indicate absence of collocation. (Scale bars: 10 μm; enlarged images, 2.5 μm.) (*B*) Quantification of the collocation of GFP-MegTmT-containing (black bars) or GFP-MegTmTΔPDZ-containing (white bars) vesicles with endogenous synectin (syn), myo6 (myo6), AP-2, and R-Tfn along the cell periphery. A total of 150 vesicles were counted from at least three cells.

crovilli, as also noted in other studies (23). In synectin-null mice, however, megalin extended along the length of the microvilli (Fig. 4*C*). A low level of megalin is normally present in microvilli (28). Therefore, the elevated presence of megalin in the microvilli of synectin-null mice most likely reflects impairment in megalin recycling caused by the loss of its interaction with myo6, rather than a complete alteration of its targeting. Neither myo6 targeting nor CCP location (Fig. 4*D*) appeared to be perturbed by the absence of synectin.

Megalin Recruits Synectin to UCV via PDZ Domain Interaction. Because VFP-syn-PDZ$^-$ was unable to associate with UCV, we tested whether a complementary approach, removal of the PBM of a synectin-binding cell surface receptor, impairs receptor trafficking by preventing synectin docking and myo6 recruitment. We used a chimeric "minireceptor" (GFP-MegTmT) where GFP is fused to the transmembrane and cytoplasmic domains of human megalin (29) and a truncated version (GFP-MegTMTΔPDZ) lacking the four-residue (DSEV) PBM, which does not bind synectin (Fig. 9*A*, which is published as supporting information on the PNAS web site). If synectin binding to the PBM is required for targeting to UCV, GFP-MegTmTΔPDZ should inhibit both synectin and myo6 recruitment to UCV.

We first sought to find whether the GFP-MegTmT minireceptor is present on the cell surface and undergoes recycling in ARPE-19 cells, similar to MDCK cells (29). Subcellular fractionation (Fig. 9*B*) and surface biotinylation (Fig. 9*C*) confirmed that both GFP-MegTmT and GFP-MegTmTΔPDZ reached the plasma membrane in ARPE-19 cells. Both were effectively endocytosed (Fig. 5*A*) and collocated to an equivalent level with the CCP marker AP-2 (data not shown) and with endocytosed R-Tfn (Fig. 5*B*). In addition, GFP-MegTmT was present in UCV, as both endogenous synectin and myo6 overlapped with GFP-MegTmT-labeled vesicles (Fig. 5 *A* and *B*). Expression of GFP-MegTmTΔPDZ reduced the ability of endogenous synectin and myo6 to associate with UCV to ≈50% of that in cells expressing GFP-MegTmT (Fig. 5 *A* and *B*). The residual association of synectin with UCV in GFP-MegTmTΔPDZ-expressing cells suggests that the population of cell surface receptors present in UCV is heterogeneous, frequently containing more than a single synectin-binding species.

Discussion

We conclude that myo6 binding to synectin depends on the engagement of synectin's PDZ domain: (*i*) although myo6 bound synectin, it did not coimmunoprecipitate with VFP-syn-PDZ$^-$, a

synectin construct that has a nonfunctional PDZ domain but still contains a potential myo6-binding site; (*ii*) expression of VFP-syn-PDZ$^-$ did not block myo6 recruitment to UCV, as would be predicted if myo6 binding to the C terminus of synectin occurred in the absence of PDZ-domain engagement; (*iii*) the binding of the myo6 tail domain to synectin *in vitro* was enhanced in the presence of a synectin PDZ ligand.

Myo6 recruitment appears to require interaction between the PBMs of engulfed receptors and synectin's PDZ domain because: (*i*) engagement of synectin's PDZ domain facilitated its binding to myo6 *in vitro*; (*ii*) the PBM of megalin was required for synectin and myo6 recruitment to megalin-containing UCV; (*iii*) megalin targeting to the apical endocytic region of proximal tubule epithelial cells, presumably a myo6-dependent process, was disrupted in kidneys of synectin-null mice, thus impairing megalin's function.

The PDZ domain may regulate myo6 binding to the C-terminal domain of synectin in two possible ways: (*i*) synectin may predominantly reside in a conformation where the PDZ domain interacts with the C terminus, physically blocking access to the myo6-binding site; (*ii*) alternatively, ligand binding to the PDZ domain may be transmitted to the C terminus by an allosteric mechanism. In either scenario, engagement of the PDZ domain would stabilize synectin in a conformation where the myo6 binding site is exposed. Thus, the PDZ domain of synectin functions as an active regulatory component conditioning myo6 binding to synectin upon synectin's association with UCV.

PDZ domains are thought to function primarily as passive binding modules (30). The only known instance of a ligand-dependent intramolecular regulation by a PDZ domain is the activation of protease activity of the bacterial protein DegS (31). Conceivably, cooperative binding mechanisms similar to the ones occurring in DegS and synectin may be more prevalent than currently appreciated.

Evidence from yeast two-hybrid assays suggests that synectin dimerization involves its N terminus (14, 21). In support, we detected by size exclusion chromatography that synectin is present as a dimer in solution under physiological conditions (data not shown). The functional significance of synectin dimerization is intriguing because a recent study suggested that myo6 exists primarily as a monomer but can dimerize when in very close proximity to another myo6 molecule (32). Myo6 dimerization was inhibited by the myo6 cargo binding domain *in vitro*, indicating that a cargo binding-dependent mechanism is required for proximity-based dimerization. It is likely that synectin dimerization, which brings two myo6 molecules in close proximity, promotes recruitment and subsequent dimerization of myo6.

Myosins I, V, VI, VII, and X participate in intracellular organelle trafficking (33), but only the cargo docking mechanism of myosin Va is well characterized (34, 35). Myosin V targeting is mediated by organelle-specific Rab GTPases, some of which bind to myosin Va directly, and some via adaptor proteins. However, this recruitment mechanism is very different from that of myo6 (Fig. 10*A*, which is published as supporting information on the PNAS web site).

Myo6 can be recruited to two distinct cargoes, UCV and CCP, although it is recruited to UCV in most cell types (8, 9). Two mechanisms modulate the ability of myo6 to target to CCP, the alternative splicing of the myo6 tail domain and the expression level of Dab2, an adapter protein that binds to clathrin, clathrin adapters, and myo6 (9). Only under conditions where Dab2 levels are high is myo6 targeting to CCP observed. Dab2 can also bind megalin (36) and as such may link megalin to myo6 in CCP. Unlike synectin, Dab2 binds to the internalization FXNPXY motif in megalin's cytoplasmic domain (36). Notably, renal proximal tubule epithelial cells from Dab2-null mice are defective in protein uptake (37), but this is due to decreased synthesis or increased turnover of megalin (38). In contrast, megalin levels remain unchanged in synectin-null mice (Fig. 4*B*).

Based on these differences, we suggest that Dab2 and synectin perform nonoverlapping functions with regards to megalin's endocytosis and transport. Dab2 likely plays a role early in endocytosis, perhaps to cluster the receptor in CCP or to signal receptor endocytosis. Synectin may act at two stages: (*i*) After the completion of endocytosis and vesicle uncoating (Fig. 10*A*), which may explain why myo6 location appeared essentially unchanged in synectin-null mice, as Dab2 could still recruit myo6 to CCP. The lack of myo6 association with UCV would be hard to discern in the dense apical endocytic region of the proximal tubule epithelial cells. (*ii*) Synectin could be required for megalin translocation down microvilli toward CCP located near the microvillus base (Fig. 10*B*). Actin filaments are oriented with their minus ends at the microvillus base, facilitating the retrograde translocation of myo6 and its cargo toward the base. Indeed, myo6 was reported to serve a similar function in the microvillar transport of the sodium proton exchanger NHE3 during acute renal hypertension (39). Loss of myo6-driven translocation may explain the redistribution of megalin seen in synectin-null mice, causing accumulation of the protein in microvilli rather than at the base of these structures.

The large and diverse group of proteins that bind to synectin's PDZ domain does not seem to have a common functional theme. The only known binding partner of synectin that does not interact with the PDZ domain is myo6. It is conceivable that this interaction underlies synectin's function, namely that synectin serves as a "universal" adapter of myo6 to a myriad of cargoes.

Materials and Methods

Expression Constructs. Expression constructs are described in detail in *Supporting Text*, which is published as supporting information on the PNAS web site.

Antibodies. Antibodies are listed in *Supporting Text*. All purchased antibodies were used at concentrations recommended by the manufacturer.

Isolation of Mouse Kidney Epithelial Cells. Kidney epithelial cells from *Snell's waltzer* mice were isolated by collagenase digestion as described in the *Supporting Text*. For immunofluorescence, cells were grown on glass coverslips coated with 50 μg/ml collagen IV (BD Biosciences, Franklin Lakes, NJ).

Fixation of Mouse Kidneys. WT and synectin-null mice (40) anesthetized by Avertin were perfused through the left ventricle with PBS and by 4% paraformaldehyde (PFA)/PBS. Kidney blocks of $\approx 2 \times 2$ mm were fixed in PBS/20 mM EGTA/4% PFA for 5 min, rinsed in PBS/20 mM EGTA, quenched in 0.05% $NaBH_4$/PBS/EGTA for 10 min, infiltrated with 1 M sucrose/PBS/EGTA for 2 h on ice, embedded in OCT (Tissue-Tek), and frozen in liquid nitrogen.

Analysis of Urine Samples. Urine pooled from three WT and three synectin-null mice was separated on 12% acrylamide gels and stained by Coomassie blue or immunoblotted for retinol-binding protein.

Uptake of R-Tfn or R-EGF. Pulse–chase and steady-state R-Tfn or R-EGF (1 μg/ml; Invitrogen, Carlsbad, CA) uptake assays were performed as described (7). Collocation of R-EGF-containing vesicles with endogenous synectin or AP-2 was quantified by counting vesicles where the corresponding fluorescence emissions overlapped. At least 50 vesicles from three different cells were quantified for each time point.

Immunofluorescence Microscopy. Cells grown on coverslips or 4-μm kidney cryosections were processed and imaged as described (7). Collocation of vesicles associated with VFP-synectin constructs and endogenous myo6 or R-Tfn was quantified as above.

GST Pull-Down Assays. GST-M6tail and polyhistidine-tagged synectin fragment (syn-120–333) were prepared as described (9, 41). ARPE-19 cells, lysed as described (7), were rotated for 1 h at 4°C in the presence of either 50 μM peptide corresponding to the C terminus of syndecan-4 (S4; RMKKKDEGSYDLGKKPIYKK-APTNEFYA; Genemed Synthesis, South San Francisco, CA) or S4 lacking the C-terminal alanine (S4Δ), thus saturating the endogenous synectin in ARPE-19 cells whose concentration was estimated by densitometric calibration (Fig. 11, which is published as supporting information on the PNAS web site) as ≈150 nM. Lysates were rotated with 40 μl of GST-M6tail coupled to glutathione-Sepharose beads (Amersham Pharmacia Biosciences, Piscataway, NJ) for 1 h at 4°C. Proteins were eluted from beads in boiling SDS/PAGE sample buffer and immunoblotted by synectin or VFP antibodies. TotalLab (Nonlinear) and Prism (GraphPad) were used for band densitometry and nonlinear regression, respectively.

Subcellular Fractionation. ARPE-19 cells grown in six-well dishes were transfected with 3 μg per well of pEGFP, pGFP-MegTmT, or pGFP-MegTmTΔPDZ and lysed 36 h after transfection in PBS/5 mM EDTA/1% Triton X-100. Pellets obtained from total cell lysate were lysed as described (7). Nuclei were removed by centrifugation for 5 min at 1,000 × *g*. Pellets produced by further centrifugation at 14,000 × *g* for 20 min comprised the plasma membrane fraction. Samples separated on 4–20% gradient SDS polyacrylamide gels were immunoblotted as described (7).

Biotinylation Assay. Cells were transfected in six-well dishes as described above and surface-labeled with EZ-link Sulfo-NHS-SS-biotin (Pierce, Rockford, IL) on ice. Surface receptors were pulled down with streptavidin beads as described (42).

We thank Drs. Sally Camper and Jill Karolyi (University of Michigan, Ann Arbor, MI) and Dr. Michael Simons (Dartmouth College) for the *Snell's waltzer* mice and synectin-null mice, Dr. Daniel Biemesderfer (Yale University, New Haven, CT) for megalin antibodies, Dr. Sandi Schmidt (Scripps Research Institute, La Jolla, CA) for AP-2 antibody, Dr. Maria Paz Marzolo (Pontificia Universidad Católica de Chile, Santiago, Chile) for the megalin minireceptor construct, and Dr. Sassan Hajmohammadi (Dartmouth College) for help with mouse kidney preparation. This work was supported by March of Dimes Birth Defects Foundation Research Grant 6-FY02-150 and by National Institutes of Health Grants EY12695 (to T.H.) and HL67960 (to A.H.).

1. Soldati, T. (2003) *Traffic* **4,** 358–366.
2. Volkmann, D., Mori, T., Tirlapur, U. K., Konig, K., Fujiwara, T., Kendrick-Jones, J. & Baluska, F. (2003) *Cell Biol. Int.* **27,** 289–291.
3. Ma, S., Fey, P. & Chisholm, R. L. (2001) *Biochim. Biophys. Acta* **1525,** 234–244.
4. Frank, D. J., Noguchi, T. & Miller, K. G. (2004) *Curr. Opin. Cell Biol.* **16,** 189–194.
5. Hasson, T. (2003) *J. Cell Sci.* **116,** 3453–3461.
6. Wells, A. L., Lin, A. W., Chen, L. Q., Safer, D., Cain, S. M., Hasson, T., Carragher, B. O., Milligan, R. A. & Sweeney, H. L. (1999) *Nature* **401,** 505–508.
7. Aschenbrenner, L., Lee, T. & Hasson, T. (2003) *Mol. Biol. Cell* **14,** 2728–2743.
8. Buss, F., Arden, S. D., Lindsay, M., Luzio, J. P. & Kendrick-Jones, J. (2001) *EMBO J.* **20,** 3676–3684.
9. Dance, A. L., Miller, M., Seragaki, S., Aryal, P., White, B., Aschenbrenner, L. & Hasson, T. (2004) *Traffic* **5,** 798–813.
10. Mishra, S. K., Keyel, P. A., Hawryluk, M. J., Agostinelli, N. R., Watkins, S. C. & Traub, L. M. (2002) *EMBO J.* **21,** 4915–4926.
11. Inoue, A., Sato, O., Homma, K. & Ikebe, M. (2002) *Biochem. Biophys. Res. Commun.* **292,** 300–307.
12. Morris, S. M. & Cooper, J. A. (2001) *Traffic* **2,** 111–123.
13. De Vries, L., Lou, X., Zhao, G., Zheng, B. & Farquhar, M. G. (1998) *Proc. Natl. Acad. Sci. USA* **95,** 12340–12345.
14. Gao, Y., Li, M., Chen, W. & Simons, M. (2000) *J. Cell Physiol.* **184,** 373–379.
15. Songyang, Z., Fanning, A. S., Fu, C., Xu, J., Marfatia, S. M., Chishti, A. H., Crompton, A., Chan, A. C., Anderson, J. M. & Cantley, L. C. (1997) *Science* **275,** 73–77.
16. Cai, H. & Reed, R. R. (1999) *J. Neurosci.* **19,** 6519–6527.
17. Lou, X., Yano, H., Lee, F., Chao, M. V. & Farquhar, M. G. (2001) *Mol. Biol. Cell* **12,** 615–627.
18. Bunn, R. C., Jensen, M. A. & Reed, B. C. (1999) *Mol. Biol. Cell* **10,** 819–832.
19. Gotthardt, M., Trommsdorff, M., Nevitt, M. F., Shelton, J., Richardson, J. A., Stockinger, W., Nimpf, J. & Herz, J. (2000) *J. Biol. Chem.* **275,** 25616–25624.
20. Avraham, K. B., Hasson, T., Steel, K. P., Kingsley, D. M., Russell, L. B., Mooseker, M. S., Copeland, N. G. & Jenkins, N. A. (1995) *Nat. Genet.* **11,** 369–375.
21. Jeanneteau, F., Diaz, J., Sokoloff, P. & Griffon, N. (2004) *Mol. Biol. Cell* **15,** 696–705.
22. Horowitz, A., Tkachenko, E. & Simons, M. (2002) *J. Cell Biol.* **157,** 715–725.
23. Lou, X., McQuistan, T., Orlando, R. A. & Farquhar, M. G. (2002) *J. Am. Soc. Nephrol.* **13,** 918–927.
24. Biemesderfer, D., Mentone, S. A., Mooseker, M. & Hasson, T. (2002) *Am. J. Physiol.* **282,** F785–F794.
25. Kozyraki, R., Fyfe, J., Verroust, P. J., Jacobsen, C., Dautry-Varsat, A., Gburek, J., Willnow, T. E., Christensen, E. I. & Moestrup, S. K. (2001) *Proc. Natl. Acad. Sci. USA* **98,** 12491–12496.
26. Leheste, J. R., Rolinski, B., Vorum, H., Hilpert, J., Nykjaer, A., Jacobsen, C., Aucouturier, P., Moskaug, J. O., Otto, A., Christensen, E. I. & Willnow, T. E. (1999) *Am. J. Pathol.* **155,** 1361–1370.
27. Christensen, E. I., Moskaug, J. O., Vorum, H., Jacobsen, C., Gundersen, T. E., Nykjaer, A., Blomhoff, R., Willnow, T. E. & Moestrup, S. K. (1999) *J. Am. Soc. Nephrol.* **10,** 685–695.
28. Biemesderfer, D., DeGray, B. & Aronson, P. S. (2001) *J. Biol. Chem.* **276,** 10161–10167.
29. Marzolo, M. P., Yuseff, M. I., Retamal, C., Donoso, M., Ezquer, F., Farfan, P., Li, Y. & Bu, G. (2003) *Traffic* **4,** 273–288.
30. Nourry, C., Grant, S. G. & Borg, J. P. (2003) *Sci. STKE* **2003,** RE7.
31. Walsh, N. P., Alba, B. M., Bose, B., Gross, C. A. & Sauer, R. T. (2003) *Cell* **113,** 61–71.
32. Park, H., Ramamurthy, B., Travaglia, M., Safer, D., Chen, L. Q., Franzini-Armstrong, C., Selvin, P. R. & Sweeney, H. L. (2006) *Mol. Cell.* **21,** 331–336.
33. Krendel, M. & Mooseker, M. S. (2005) *Physiology (Bethesda)* **20,** 239–251.
34. Fukuda, M., Kuroda, T. S. & Mikoshiba, K. (2002) *J. Biol. Chem.* **277,** 12432–12436.
35. Wu, X. S., Rao, K., Zhang, H., Wang, F., Sellers, J. R., Matesic, L. E., Copeland, N. G., Jenkins, N. A. & Hammer, J. A., III (2002) *Nat. Cell Biol.* **4,** 271–278.
36. Oleinikov, A. V., Zhao, J. & Makker, S. P. (2000) *Biochem. J.* **347,** 613–621.
37. Morris, S. M., Arden, S. D., Roberts, R. C., Kendrick-Jones, J., Cooper, J. A., Luzio, J. P. & Buss, F. (2002) *Traffic* **3,** 331–341.
38. Nagai, J., Christensen, E. I., Morris, S. M., Willnow, T. E., Cooper, J. A. & Nielsen, R. (2005) *Am. J. Physiol.* **289,** F569–F576.
39. Yang, L. E., Maunsbach, A. B., Leong, P. K. & McDonough, A. A. (2005) *J. Am. Soc. Nephrol.* **16,** 2890–2896.
40. Chittenden, T. W., Claes, F., Lanahan, A. A., Autiero, M., Palac, R. T., Tkachenko, E. V., Elfenbein, A., Ruiz de Almodovar, C., Dedkov, E., Tomanek, R., *et al.* (2006) *Dev. Cell* **10,** 783–795.
41. Hasson, T. & Mooseker, M. S. (1994) *J. Cell Biol.* **127,** 425–440.
42. Swiatecka-Urban, A., Boyd, C., Coutermarsh, B., Karlson, K. H., Barnaby, R., Aschenbrenner, L., Langford, G. M., Hasson, T. & Stanton, B. A. (2004) *J. Biol. Chem.* **279,** 38025–38031.